Reorientational dynamics of NaBH4 and KBH4

ARTICLE *in* THE JOURNAL OF PHYSICAL CHEMISTRY C · JUNE 2010

Impact Factor: 4.77 · DOI: 10.1021/jp1006473

Reorientational Dynamics of $NaBH_4$ and KBH_4

Nina Verdal,*,† Michael R. Hartman,‡ Timothy Jenkins,† Daniel J. DeVries,§ John J. Rush,†,∥ and Terrence J. Udovic†

NIST Center for Neutron Research, National Institute of Standards and Technology, Gaithersburg, Maryland 20899-6102, Nuclear Engineering and Radiological Sciences, University of Michigan, Ann Arbor, Michigan 48109-2104, Radiation and Isotopes for Health, Delft University of Technology, Mekelweg 15, 2629 JB Delft, The Netherlands, and Department of Materials Science and Engineering, University of Maryland, College Park, Maryland 20742-2115

Received: January 22, 2010; Revised Manuscript Received: April 12, 2010

The details of the rotational dynamics of borohydride ions in both the ordered and disordered crystal phases of $NaBH_4$ and in the disordered crystal phase of KBH_4 were determined by quasielastic neutron scattering (QNS). Model fits of the QNS data indicate that the BH_4^- tetrahedron in the ordered phase of $NaBH_4$ rotates with a combination of 2-site and 3-site reorientations that preserve its crystallographic orientation. The QNS results for the disordered phases are well described by a model assuming nearest-neighbor BH_4^- jumps from one corner to another of a cube formed by eight hydrogen positions of half occupancy. Distinguishing between likely mechanisms for reorientation was made possible by collecting data at sufficiently high momentum transfer. The activation energies derived for the low-temperature and high-temperature phases of $NaBH_4$ are 13.4 ± 0.8 and 11.9 ± 0.5 kJ/mol, respectively. We find an activation energy for KBH_4 of 14.6 ± 0.5 kJ/mol in the high-temperature phase. The torsional vibration bands of both borohydrides were also measured by inelastic neutron scattering.

Introduction

The alkali borohydrides are one class of material currently being evaluated for suitability as an on-board storage medium for hydrogen in vehicular fuel cells. They are solids at room temperature and contain a high volumetric hydrogen density (121.3 kg/m^3 for $LiBH_4$, 113.1 kg/m^3 for $NaBH_4$, and 87.5 kg/m^3 for KBH_4) and a high gravimetric hydrogen density (18.4 mass % for $LiBH_4$, 10.6 mass % for $NaBH_4$, and 7.4 mass % for KBH_4). Thus, in principle, they exceed current goals for hydrogen storage capacities.

Their stability at room temperature is a potential advantage, since no external cryogenic cooling is needed as with physisorbed H_2, but the temperatures required to dehydrogenate alkali borohydrides are substantial. Dehydrogenation occurs only above the borohydride melting point, which is 505 °C for $NaBH_4$ and 585 °C for KBH_4.[1] Although $LiBH_4$ is the most promising of the alkali borohydrides for these applications, rehydrogenation and cycling of $LiBH_4$ occurs slowly and incompletely.[2]

The development of methods to destabilize metal hydrides in order to make them viable is an active field of research.[3−7] Through doping, catalysis, nanoconfinement, or alloying, more favorable dehydrogenation and rehydrogenation reactions may be developed. Vajo et al.[4] point out that the B−H bond is very strong and directional and possesses high activation barriers to atomic motion. All of these characteristics diminish the reactivity of the BH_4^- anion. An interesting additional aspect of borohydride properties is the propensity of the BH_4^- anion to undergo rotational motions within the crystal lattice. A thorough characterization of BH_4^- dynamical behavior in the neat borohydride compounds is required to understand how this behavior is perturbed by the various modification methods such as nanoconfinement and whether there is any relationship between such rotational perturbations and hydrogen-cycling properties. Below a certain phase-transition temperature, ≈190 K for $NaBH_4$ and between 65 and 70 K for KBH_4, both borohydrides possess an ordered structure[8,9] with tetragonal symmetry in space group $P4_2/nmc$. Above this temperature, both borohydrides form a cubic phase in space group $Fm-3m$, which is distinguished by the disordering of the hydrogen atoms onto the eight corners of a cube, each with half occupancy.[8−11]

In this paper we present the results of quasielastic and inelastic neutron scattering studies of $NaBH_4$ and KBH_4 to reveal the details of reorientation vs temperature and the vibrational density of states. The activation energies for the rotational dynamics of the BH_4^- hydrogen atoms are determined. We further provide models characterizing the nature of the reorientations and the jump distances for the low-temperature phase of $NaBH_4$ and the high-temperature phases of $NaBH_4$ and KBH_4 that are compared to our and others' observations[12] and previous diffraction results.[8,9]

Materials and Methods

All neutron scattering measurements were performed at the NIST (National Institute for Standards and Technology) Center for Neutron Research (NCNR). The hydrogen isotope ^{1}H has a much higher cross section for neutron scattering than that of other isotopes. Neutron scattering spectra are therefore dominated by the motions of any ^{1}H present in the sample, making it an ideal tool to study the dynamics of hydrogen atoms. Neutron vibrational spectra were collected using the filter-analyzer neutron spectrometer (FANS)[13] with a Cu(220) monochromator and 20 min of arc for both the pre- and postmonochromator collimations. Data were collected over the energy

* Corresponding author. E-mail: nina.verdal@nist.gov.
† National Institute of Standards and Technology.
‡ University of Michigan.
§ Delft University of Technology.
∥ University of Maryland.

10.1021/jp1006473
Published on Web 05/10/2010

range of 34−200 meV or 272−1600 cm^{-1} at 4 K and at temperatures just below and above the order−disorder phase transition.

The quasielastic measurements were performed on the high flux backscattering spectrometer (HFBS)[14] and the time-of-flight disc chopper spectrometer (DCS).[15] HFBS data were collected for a series of temperatures between 150 and 220 K for $Na^{11}BH_4$ and between 128 and 220 K for $K^{11}BH_4$. DCS data were collected for a series of temperatures between 260 and 400 K for $Na^{11}BH_4$ and between 185 and 325 K for $K^{11}BH_4$. At lower temperatures, the reorientational dynamics are sufficiently slow as to be unobservable by these instruments.

Isotopically labeled boric acid (99 at % ^{11}B) was used to synthesize the sodium borohydride ($Na^{11}BH_4$) according to a previously published method.[16] The labeled sodium borohydride was used as a precursor to potassium borohydride ($K^{11}BH_4$) production. The potassium borohydride was synthesized by the metathesis reaction of sodium borohydride with potassium hydroxide at room temperature in distilled water. In each case, the final product was purified using solvent extraction and washing, and the purity was verified through FT-IR and XRD measurements. The isotopic labeling of boron is necessary in order to reduce the neutron absorption of the sample. Naturally occurring boron is approximately 20% ^{10}B and 80% ^{11}B. The neutron absorption cross-section for ^{10}B is 7 orders of magnitude greater than that of ^{11}B, and the elimination of the ^{10}B isotope from the sample increases neutron transmission considerably.

The data reported here were collected from powder that was contained in an aluminum foil packet and shaped into either an annular or flat-plate geometry inside a cylindrical aluminum can. These sample cans were sealed in a He-atmosphere glovebox and subsequently placed in a He closed-cycle refrigerator for neutron measurements. The flat samples, because they contained less material and the neutrons passed through the sample only once, do not exhibit observable effects of multiple scattering, in contrast to the annular samples, which display some minor multiple scattering at the lowest momentum transfers (Q).

Results and Analysis

Typical HFBS and DCS spectra consisted of an elastic peak and a broader quasielastic component, centered at the elastic peak, resulting from the transfer of energy between the incident neutron and the rotating BH_4^- anions. At each temperature, the data were reduced and analyzed as a function of momentum transfer.[17] Some of these data are presented in Figures 1, 5, and 7. The resolution function (resulting only from elastic scattering) was obtained at low temperature (below 30 K) where there are no observable hydrogen dynamics on the time scale accessible by these instruments. The data were analyzed in two ways. In one approach, each spectrum was fit to a delta function (elastic scattering), a Lorentzian function (quasielastic scattering), and a linear background. The delta and Lorentzian functions were convolved with the resolution function. This is a general treatment and will be referred to as the QNS model. The derived mean Lorentzian line width over all Q values was used in an Arrhenius fit. The fitted data itself was used to obtain the elastic incoherent structure factor.

The Q-dependent, elastic incoherent structure factor (EISF) is the ratio of the elastic peak area (A_0) to the sum of elastic and quasielastic peak areas (A_1)

$$\mathrm{EISF} = \frac{A_0}{A_0 + A_1} \tag{1}$$

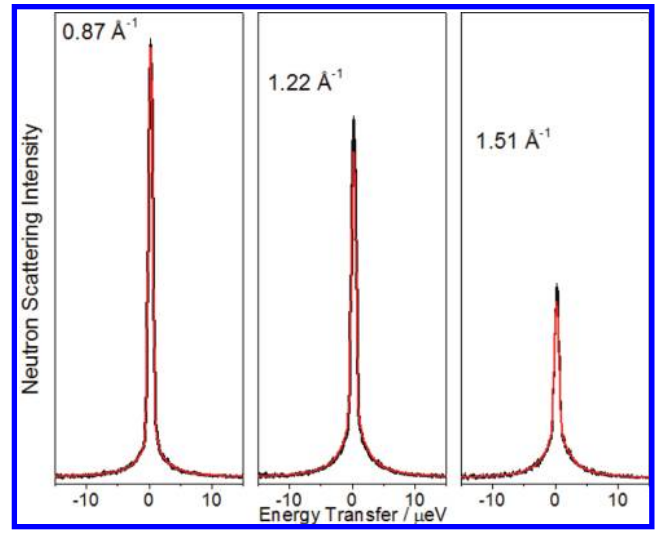

Figure 1. Representative quasielastic spectra for the low temperature phase of $NaBH_4$ at 180 K for momentum transfers Q = 0.87, 1.22, and 1.51 Å^{-1} (black) compared with the convolved 2- and 3-site jump model (red), representing the likely reorientation dynamic.

in which A_0 and A_1 are related to the scattering function $S(Q,\omega)$ by

$$S(Q,\omega) = A_0\delta(\omega) + A_1\frac{1}{\pi}\left(\frac{\frac{1}{\tau}}{\left(\frac{1}{\tau}\right)^2 + \omega^2}\right) \tag{2}$$

in a simple model in which the quasielastic contribution to the line shape can be represented by a single Lorentzian with a hwhm of $1/\tau$.

In a second approach to the data analysis, the area and line shape are fit with a function representing one of several possible jump models. The parameters in the fit are: jump distance, total area, and width of Lorentzian(s) meant to represent the quasielastic scattering. A resolution function is used here as well. Many of the jump models require the presence of more than one Lorentzian, dependent on one or more residence times τ. Because of the model-specific constraints imposed on the equation describing $S(Q,\omega)$, this approach provides the best way to compare a reorientation mechanism with the observed data, which is done by the comparison of χ^2 values.

The diffusion of hydrogen by a series of jumps was first proposed by Chudley and Elliott.[18] Modeling of jump dynamics assumes that the contributions to the incoherent structure factor $S(Q,\omega)$ such as vibration, rotation, and translation are separable under the experimental conditions. Thus the molecule of interest vibrates at the bottom of the potential energy well at least an order of magnitude longer than the time between (essentially) instantaneous jumps to the adjacent potential energy well. For this libration, the period of oscillation is roughly 0.1 ps. At the highest temperatures for which quasielastic data was recorded, the line width corresponds to roughly 1 ps. Therefore, at the highest temperatures for which data were collected, there are over 10 librations for every jump along the potential energy surface, and therefore the assumed conditions for which the Chudley-Elliot model hold are valid.

Reorientational Dynamics

Ordered Low-Temperature Phase. The BH_4^- group rotational dynamics in $NaBH_4$ has been investigated at temperatures

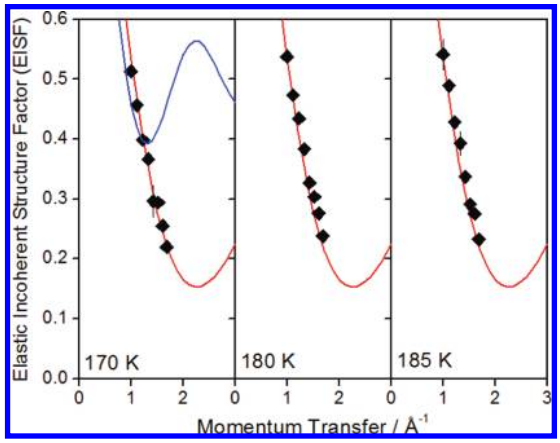

Figure 2. Experimental EISF for the low temperature phase of $NaBH_4$ compared with two possible jump models: a 3-site jump (blue) and a convolution of 2- and 3-site jumps (red). The models use relevant jump distances corresponding to the crystal geometry at 4 K. Error bars are obscured by the graph symbol and represent one standard deviation.

both above and just below the phase transition at 190 K. Diffraction data[9] reveals that in the low-temperature phase, the hydrogen atoms of the BH_4^- anion occupy four tetrahedral positions. A number of models for reorientational jumps were used to fit the data as shown in Figures 1 and 2. The model that provides the best fit is a convolution of a two-site and three-site jump model[19] as derived in the Supporting Information. The scattering function $S(Q,\omega)$ used to describe this is[20]

$$S(Q,\omega) = \frac{1}{4}\Bigg[(1 + j_0(Qa))(1 + j_0(Qa))\delta(\omega) + (1 + j_0(Qa))(1 - j_0(Qa))\frac{1}{\pi}\frac{\left(\frac{3}{2\tau_3}\right)}{\left(\frac{3}{2\tau_3}\right)^2 + \omega^2} + (1 + j_0(Qa))(1 - j_0(Qa))\frac{1}{\pi}\frac{\left(\frac{2}{\tau_2}\right)}{\left(\frac{2}{\tau_2}\right)^2 + \omega^2} + (1 - j_0(Qa))(1 - j_0(Qa))\frac{1}{\pi}\frac{\left(\frac{2}{\tau_2} + \frac{3}{2\tau_3}\right)}{\left(\frac{2}{\tau_2} + \frac{3}{2\tau_3}\right)^2 + \omega^2}\Bigg] \quad (3)$$

in which $j_0(x) = (\sin x)/x$ is a zeroth-order spherical Bessel function of the first kind and accounts for the isotropic orientation of the crystals in a powder sample. a is the distance between jump sites, $\hbar\omega$ is the energy transfer from the sample to the neutron, and τ_i is the average residence time between i equivalent jump sites, which is determined from the width of the Lorentzian used to simulate the quasielastic scattering features. According to the above scattering function for simultaneous 2- and 3-site hydrogen jumps, a schematic of which is presented in Figure 3, the quasielastic scattering should be fit with three Lorentzian functions of different linewidths, related to two τ_i values. A good fit to this equation was attained by restricting τ_2 and τ_3 to equivalent values. This assumes that the activation energy and attempt frequency for the 2-site jump is

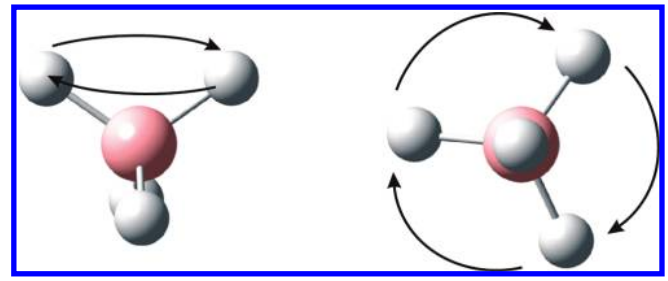

Figure 3. Schematic of the 2-site and 3-site jump.

equivalent to that for the 3-site jump within our experimental error. Consistent with this assumption, the data fits a simple quasielastic model well with only one Lorentzian and the resulting Arrhenius plot is quite linear (see Figure 9 and the relevant discussion). Additionally, previous NMR studies[21−23] have found only one activation energy for the reorientation dynamics of this phase.

The observed EISF is fit to that of the convolved 2-site and 3-site jump model for an isotropic polycrystalline sample (see Figure 2)

$$\mathrm{EISF} = \frac{1}{4}[(1 + j_0(Qa))(1 + j_0(Qa))] \quad (4)$$

where the jump distance $a = 1.99$ Å for $NaBH_4$. Although a simple 3-site jump model is physically reasonable and requires only one Lorentzian, the EISF for this model is in poor agreement with the observed data. For this system, the 2-site jump, which is also a reasonable mechanism for reorientation, has an equivalent EISF to the 3-site jump. The disagreement between the observed EISF and that for either the 3-site jump or the 2-site jump is so extreme (see Figure 2) that those mechanisms can be clearly eliminated as possibilities. A simultaneous 3-site and 4-site jump model is also a good fit to the observed data but is physically inconsistent with the crystallographic data. A model in which hydrogen atoms jump with equal probability among four equivalent proton sites of a tetrahedron may also be in reasonable agreement with the data. Unfortunately, we are unable to rule out the most plausible models for reorientation given the limited Q range over which this data was collected. Data at higher Q were not collected at these lower temperatures with narrow quasielastic linewidths: Shorter incident neutron wavelengths are required for a larger momentum transfer, and unfortunately provide broader resolution widths. This restriction makes our result for the reorientation mechanism present in the ordered phase of $NaBH_4$ less certain.

Disordered High-Temperature Phase. Diffraction studies[8,9] show a change in the ordering of the BH_4^- hydrogen atoms upon undergoing the phase transition in both $NaBH_4$ and KBH_4. The hydrogen atoms remain in a tetragonal arrangement about the boron, but the hydrogen atoms in the high-temperature phase are equally likely to be found at the eight corners of a cube surrounding the boron atom as depicted in Figure 4. One way to jump from one orientation of the BH_4^- tetrahedron to another orientation is by rotating about a 4-fold axis of this cube. This corresponds to hydrogen jump distances of 1.41 and 1.39 Å for $NaBH_4$ and KBH_4, respectively, using bond lengths and angles from crystallographic data at 4 K.[9] The data obtained can be modeled with an EISF for jumps about any of the three 4-fold axes (see Figures 6 and 8), allowing hydrogen atoms to visit the eight corners of a cube[24]

$$\mathrm{EISF} = \frac{1}{8}[1 + 3j_0(Qa) + 3j_0(\sqrt{2}Qa) + j_0(\sqrt{3}Qa)] \quad (5)$$

where a is now the hydrogen jump distance around the 4-fold rotational axis. In this model, the quasielastic feature is represented by three Lorentzian functions (L_i), all of different widths, each related to the same time constant τ and of the form

$$L_1 = \frac{1}{\pi}\left(\frac{\frac{2}{3}\tau}{\omega^2 + \left(\frac{2}{3}\tau\right)^2}\right) \quad (6)$$

$$L_2 = \frac{1}{\pi}\left(\frac{\frac{4}{3}\tau}{\omega^2 + \left(\frac{4}{3}\tau\right)^2}\right) \quad (7)$$

$$L_3 = \frac{1}{\pi}\left(\frac{\frac{2}{\tau}}{\omega^2 + \left(\frac{2}{\tau}\right)^2}\right) \quad (8)$$

This model was originally developed to describe possible reorientations of the S−H ion in NaSH and CsSH along the [111] direction of the unit cell.[24] We will refer to this as the [111] jump model.

The EISF can be very useful in determining the reorientation mechanism and jump distance of hydrogen atoms in these systems. However, at small momentum transfer, the EISF functions for various mechanisms are virtually indistinguishable. For example, the EISF for isotropic rotational diffusion[19] ($j_0^2(Qr)$ where r is the BH bond length) is essentially identical to the [111] jump model at low Q up to the first minimum of the function, which for this system is ~2.5 Å^{-1}. A previously published[12] EISF for the high temperature phase of $NaBH_4$ contains data up to but not above this Q value. However, only at momentum transfers above this value do the two functions diverge, as seen in Figures 6 and 8. Collecting data at higher momentum transfer is essential to test which reorientation mechanism fits the data, especially when comparing two physically different but reasonable models. Thus our results allow a clear choice of the [111] reorientation model for the high temperature borohydride phases, not possible in previous work.[12]

Activation Energy and Residence Times. The quasielastic line width as a function of temperature was fit to an Arrhenius equation: $\ln(1/\tau) = \ln(1/\tau_0) - E_a/(kT)$ for each of the crystal

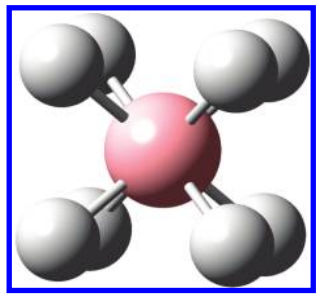

Figure 4. BH_4^- ion as described crystallographically with half-occupancy hydrogen positions.

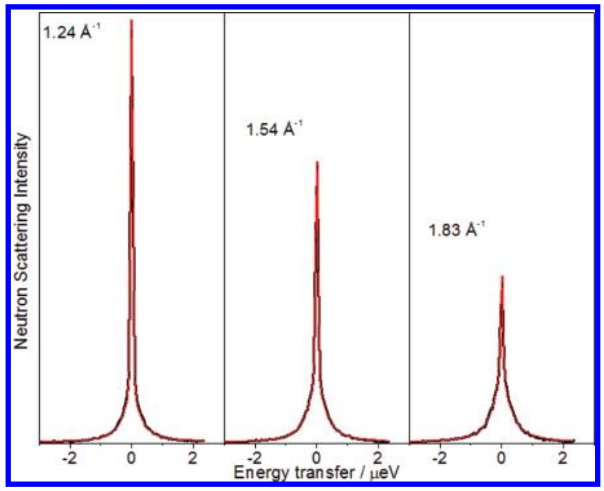

Figure 5. Representative quasielastic neutron scattering spectra of the high temperature phase of $NaBH_4$ at 300 K with 5 Å incident neutrons. Data (black) are shown at three momentum transfers: Q = 1.24, 1.54, and 1.83 Å^{-1} and compared with simulations for the [111] model (red), for reorientation about a C_4 axis.

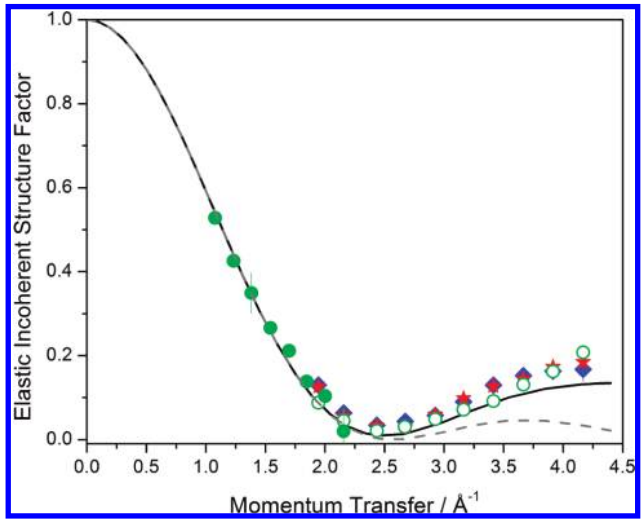

Figure 6. Shown are the observed EISF points for $NaBH_4$ at 300 K using 5 Å incident neutrons (filled green circles) and at 300 (empty green circles), 350 (blue diamonds), and 400 K (red stars) with 2.75 Å incident neutrons. These points are compared to the [111] model for hydrogen reorientation from one corner of a cube to an adjacent corner of the cube, rotating about a C_4 axis (solid black line). The EISF for isotropic rotational diffusion is the dashed gray line. Error bars may be obscured by symbols and represent one standard deviation.

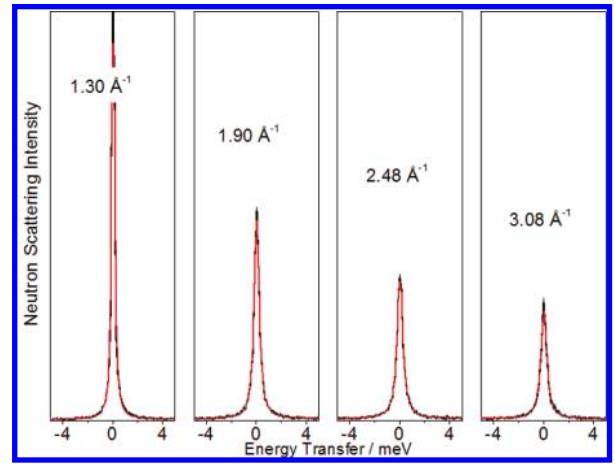

Figure 7. Representative quasielastic neutron scattering data of KBH_4 at 325 K, with 2.75 Å incident neutrons. Data (black) are shown as a function of momentum transfer and compared with the [111] 4-fold reorientation model (red).

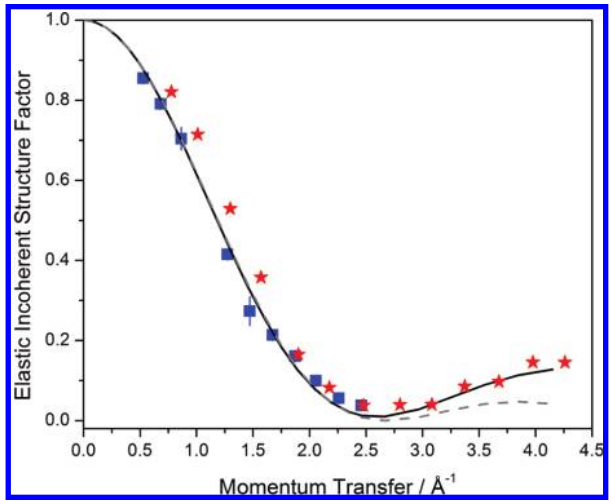

Figure 8. Observed EISF for KBH_4 at 320 K, using 4.1 Å incident neutrons (blue squares) and at 325 K with 2.75 Å incident neutrons (red stars). These points are compared to a model for hydrogen reorientation from one corner of a cube to an adjacent corner of the cube, rotating about a C_4 axis (solid black line). The EISF for isotropic rotational diffusion is the dashed gray line. Error bars may be obscured by symbols and represent one standard deviation.

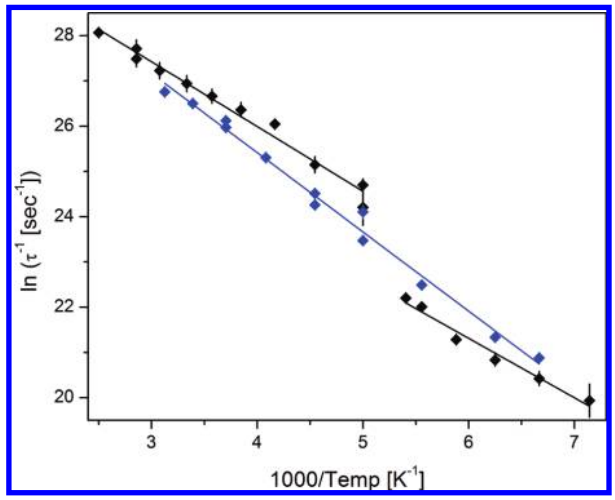

Figure 9. Arrhenius plot for $NaBH_4$ (black) and KBH_4 (blue). Quasielastic linewidths are plotted over the temperature range of 400 to 150 K. Error bars represent one standard deviation.

phases in order to obtain an activation energy E_a and pre-exponential factor τ_0 for the BH_4^- reorientations (see Figure 9). Data collected over the range of 150 to 185 K for the low-temperature phase of $NaBH_4$ yield an activation energy of 13.4 ± 0.8 kJ/mol with an estimated pre-exponential factor τ_0 of 38 fs. An Arrhenius plot using τ calculated from a fit to the convolved 2-site and 3-site jump model gives values of 16.7 ± 0.7 kJ/mol and 6 ± 3 fs. Previous NMR studies for this phase reported activation energies of 14.8,[23] and 15.3,[22] and most recently 14.6 kJ/mol.[21] An energy barrier V_0 (where $V_0 = E_a + (1/2)\hbar\omega$) of 10.1 kJ/mol was also determined from NMR studies.[25]

From data collected from 200 to 400 K, the activation energy for the high-temperature phase of $NaBH_4$ was determined to be 11.9 ± 0.5 kJ/mol with a τ_0 of 17 ± 4 fs. This activation energy is similar to those reported in previous NMR (12.1,[23] 14.8,[22] and 11.3 kJ/mol[21]), Raman[26] (12.1 kJ/mol), and quasielastic neutron scattering[12] (11.3 kJ/mol) studies. A prior inelastic neutron scattering study[27] derived energy barriers of 20.4 and 16.7 kJ/mol from BH_4^- torsional band frequencies. A smaller

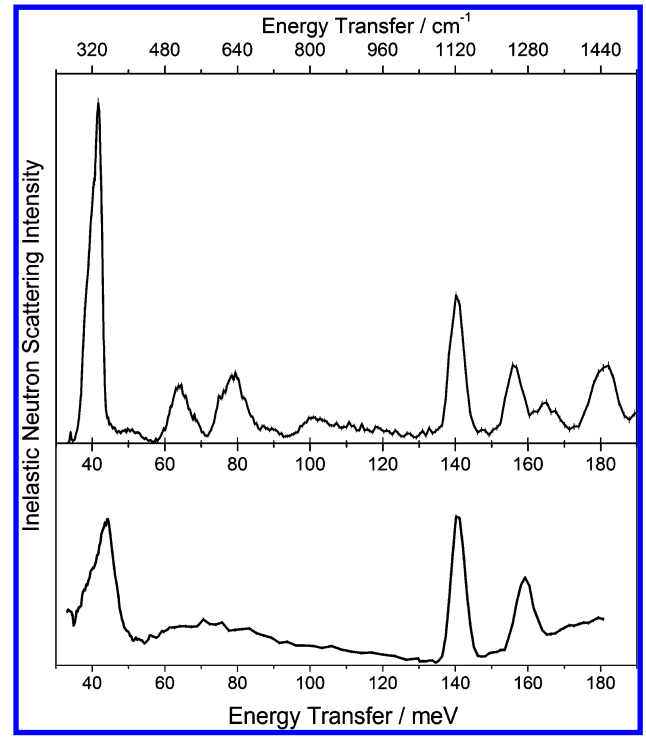

Figure 10. Neutron vibrational spectra of KBH_4 (top) and of $NaBH_4$ (bottom) collected at 4 K. The KBH_4 libration peak sits at 42 meV (339 cm^{-1}) with a fwhm of 4 meV. The $NaBH_4$ libration peak is at 44 meV (355 cm^{-1}) with a fwhm of 8 meV. Error bars represent one standard deviation. Combination bands involving the libration mode are found at 64, 78, and 182 meV for KBH_4 but are not resolved in the $NaBH_4$ spectrum. The peaks at 140, 156 (KBH_4), 140, and 159 meV ($NaBH_4$) have been assigned[28] as fundamentals for bending modes.

activation energy of 9.3 ± 0.3 kJ/mol and τ_0 equal to 19 ± 2 fs was determined from a fit of the quasielastic spectra to the [111] model.

In the case of KBH_4, an Arrhenius fit to the Lorentzian line width from BH_4^- jump reorientations in the high-temperature phase from 140 to 320 K yields an activation energy of 14.2 ± 0.5 kJ/mol. Values of 15.3 ± 0.5 kJ/mol and 2.7 ± 0.7 fs were obtained by a fit of the spectra to the [111] model for hydrogen reorientation. Both of these values compare well with other results. NMR studies find activation energies of 14.8[23] and 15.5 kJ/mol[21] and a barrier height of 15.7 kJ/mol.[25] In another study, a barrier for reorientation of 9.2 kJ/mol was derived from the widths of the υ_2 bending mode in a nonresonant Raman spectrum as a function of temperature from 308 to 500 K.[26]

Librations of the Borohydrides. The peak of the $NaBH_4$ and KBH_4 librational bands at 4 K occur at 44 meV (355 cm^{-1}) and 42 meV (339 cm^{-1}), respectively (see Figure 10). Assignments for these and other fundamental vibrations of $NaBH_4$ and KBH_4 have been published previously.[28] The width of the $NaBH_4$ band (~8 meV fwhm) is twice that of KBH_4 (~4 meV fwhm), possibly reflecting more phonon dispersion among BH_4^- anions within the smaller $NaBH_4$ lattice. The two KBH_4 combination bands at 64 and 79 meV with contributions from the libration mode are quite sharp, consistent with the width of the fundamental. Similarly, the corresponding $NaBH_4$ combination bands are broadened so as to be indistinguishable, consistent with the broad $NaBH_4$ libration fundamental.

For KBH_4, the librational band intensity decreases and the shape changes as the temperature is raised, partly due to the Debye−Waller factor. Yet, across the phase transition, an abrupt change is observed in the torsional spectrum and Debye−Waller

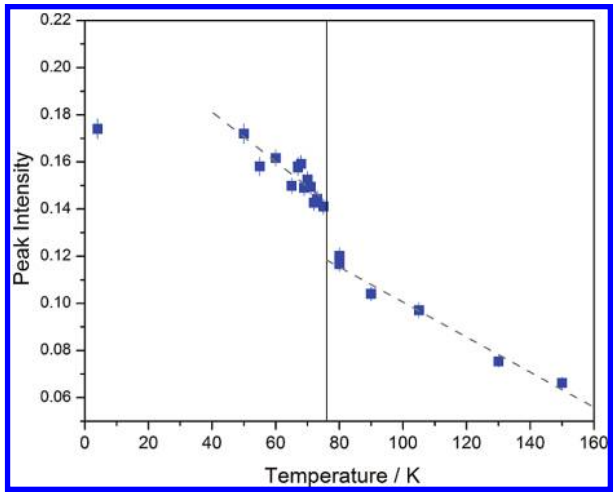

Figure 11. Plot of the intensity at the peak of the KBH_4 librational feature as a function of temperature. The dashed lines are guides to the eye. The intensity of the peak drops suddenly across the order−disorder phase transition (shown with a vertical line). Error bars represent one standard deviation.

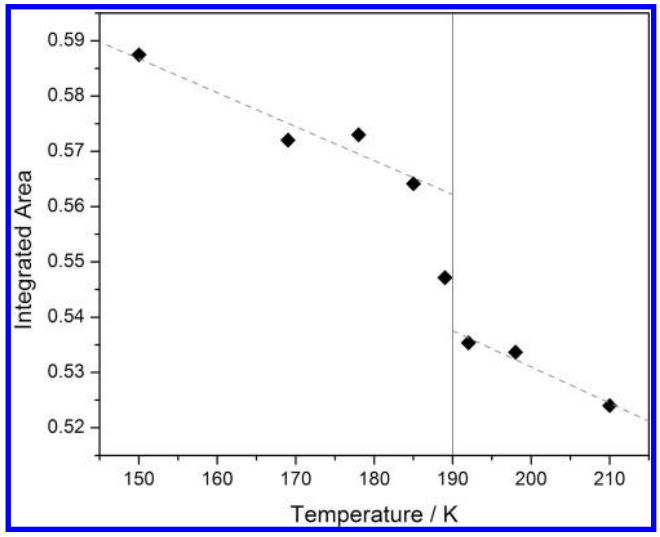

Figure 12. Plot of the integrated area of the $NaBH_4$ librational band as a function of temperature. Dashed lines are guides to the eye. The intensity drops suddenly over the range of the order−disorder phase transition (shown with a solid vertical line).

factor that suggest a change in the character of the libration potential (see Figure 11). For $NaBH_4$, at temperatures just below the relatively higher 190 K phase transition, much of the structure present in the librational band at 4 K has already broadened. However, the integrated intensity of the librational band falls sharply across the phase transition, again signaling a step increase in the Debye−Waller factor (see Figure 12). This coincides with the order−disorder crystallographic transition and a change in the reorientation attempt frequency ($1/\tau_0$) and the mechanism for reorientation, as determined from the quasielastic neutron scattering results.

Summary and Conclusions

Neutron vibrational and quasielastic spectra have been measured on isotopically enriched samples of $K^{11}BH_4$ and $Na^{11}BH_4$. Observed changes in the BH_4^- librational band across the phase transition imply a change in the nature of the librational potential energy surface, which governs the BH_4^- reorientation dynamics.

Quasielastic neutron scattering has been measured for the $Na^{11}BH_4$ low-temperature (ordered) and high-temperature (disordered) phase as well as for the isostructural $K^{11}BH_4$ high-temperature (disordered) phase. The BH_4^- reorientation mechanism for the high-temperature phase of both $NaBH_4$ and KBH_4 has been interpreted as jumps around any of the three 4-fold (C_4) axes, restricting the hydrogen positions to the eight corners of a cube, with a jump distance of 1.41 ($NaBH_4$) and 1.39 Å (KBH_4), consistent with crystallographic observations. The activation energies for reorientation in the high-temperature phases of $NaBH_4$ and KBH_4 were found to be 11.9 ± 0.5 and 14.6 ± 0.5 kJ/mol, respectively. The EISF of the low-temperature $NaBH_4$ phase is in agreement with a model that incorporates both 2-site and 3-site jumps over a distance of 1.99 Å. This model is consistent with the tetragonal symmetry found in the low-temperature phase by diffraction.[9] The activation energy for reorientation was estimated to be 13.4 ± 0.8 kJ/mol under the assumption that the 2- and 3-site jumps have equivalent energies.

The equations used to model jump dynamics can have very similar results at low Q. As pointed out by Lechner,[29] in order to rule out one model in favor of another, data must be collected at higher Q values, where these functions diverge. In the case of the borohydrides, at Q values below 2.5 $Å^{-1}$, the models for isotropic rotational diffusion and for jumps to the eight corners of a cube are indistinguishable. Only at $Q > 2.5$ $Å^{-1}$ is one able to determine the relevance of one model over another.

Acknowledgment. This work utilized facilities supported in part by the National Science Foundation under Agreement No. DMR-0454672. This work was partially supported by the DOE through Award No. DE-AI-01-05EE11104 within the EERE-supported Metal Hydride Center of Excellence. We thank Taner Yildirim for helpful discussions.

Supporting Information Available: Detailed derivation of the scattering function $S(Q,\omega)$ for the simultaneous 2-site and 3-site jump model. This material is available free of charge via the Internet at http://pubs.acs.org.

References and Notes

(1) Züttel, A.; Borgschulte, A.; Orimo, S.-I. *Scr. Mater.* **2007**, *56*, 823–828.
(2) Mauron, P.; Buchter, F.; Friedrichs, O.; Remhof, A.; Bielmann, M.; Zwicky, C. N.; Zuttel, A. *J. Phys. Chem. B* **2008**, *112*, 906–910.
(3) Vajo, J. J.; Mertens, F.; Ahn, C. C.; Bowman, R. C.; Fultz, B. *J. Phys. Chem. B* **2004**, *108*, 13977–13983.
(4) Vajo, J. J.; Olson, G. L. *Scr. Mater* **2007**, *56*, 829–834.
(5) Vajo, J. J.; Salguero, T. T.; Gross, A. F.; Skeith, S. L.; Olson, G. L. *J. Alloy Compd.* **2007**, *446−447*, 409–414.
(6) Gross, A. F.; Vajo, J. J.; Atta, S. L. V.; Olson, G. L. *J. Phys. Chem. C* **2008**, *112*, 5651–5657.
(7) Nakamori, Y.; Orimo, S.-i. *J. Alloys Compd.* **2004**, *370*, 271–275.
(8) Fisher, P.; Züttel, A. *Mater. Sci. Forum* **2004**, *443−444*, 287–290.
(9) Renaudin, G.; Gomes, S.; Hagemann, H.; Keller, L.; Yvon, K. *J. Alloys Compd.* **2004**, *375*, 98–106.
(10) Luck, R. L.; Schelter, E. J. *Acta Crystallogr.* **1999**, *C55*, IUC9900151.
(11) Davis, R. L.; Kennard, C. H. L. *J. Solid State Chem.* **1985**, *59* (3), 393.
(12) Remhof, A.; Łodziana, Z.; Buchter, F.; Martelli, P.; Pendolino, F.; Friedrichs, O.; Züttel, A.; Embs, J. P. *J. Phys. Chem. C* **2009**, *113*, 16834–16837.
(13) Udovic, T. J.; Brown, C. M.; Leão, J. B.; Brand, P. C.; Jiggetts, R. D.; Zeitoun, R.; Pierce., T. A.; Peral, I.; Copley, J. R. D.; Huang, Q.; Neumann, D. A.; Fields, R. J. *Nucl. Instrum. Methods A* **2008**, *588*, 406–413.
(14) Meyer, A.; Dimeo, R. M.; Gehring, P. M.; Neumann, D. A. *Rev. Sci. Instrum.* **2003**, *74*, 2759.
(15) Copley, J. R. D.; Cook, J. C. *Chem. Phys.* **2003**, *292*, 477.
(16) Hartman, M. R.; Rush, J. J.; Udovic, T. J.; Bowman, R. C.; Hwang, S.-J. *J. Solid State Chem.* **2008**, *180*, 1298–1305.

(17) Azuah, R.; Kneller, L.; Qiu, Y.; Tregenna-Piggott, P. L. W.; Brown, C.; Copley, J.; Dimeo, R. *J. Res. NIST* **2009**, *114* (6), 341–358.
(18) Chudley, C. T.; Elliott, R. J. *Proc. Phys. Soc. London* **1961**, *77*, 353–361.
(19) Bée, M. *Quasielastic Neutron Scattering, Principles and Applications in Solid State Chemistry, Biology and Materials Science*; Adam Hilger: Bristol, 1988.
(20) Hartman, M. R. to be published.
(21) Babanova, O. A.; Soloninin, A. V.; Stepanov, A. P.; Skripov, A. V.; Filinchuk, Y. *J. Phys. Chem. C* **2010**, *114* (8), 3712–3718.
(22) Tarasov, V. P.; Bakrum, S. I.; Privalov, V. I.; Shamov, A. A. *Russ. J. Inorg. Chem.* **1990**, *35*, 1195–1197.
(23) Tsang, T.; Farrar, T. C. *J. Chem. Phys.* **1969**, *50* (8), 3498.
(24) Rush, J. J.; Graaf, L. A. d.; Livingston, R. C. *J. Chem. Phys.* **1973**, *58* (8), 3439–3447.
(25) Ford, P. T.; Richards, R. E. *Discuss. Faraday Soc.* **1955**, *19*, 230–238.
(26) Hagemann, H.; Gomes, S.; Renaudin, G.; Yvon, K. *J. Alloys Compd.* **2004**, *363*, 126–129.
(27) Tomkinson, J.; Waddington, T. C. *J. Chem. Soc. Faraday Trans. II* **1976**, *72* (2), 528–538.
(28) Allis, D. G.; Hudson, B. S. *Chem. Phys. Lett.* **2004**, *385*, 1660172.
(29) Lechner, R. E.; Heidemann, A. *Commun. Phys.* **1976**, *1*, 213–221.

JP1006473